Chapter 5. Ediacaran stratigraphic reconstruction of Yangtze platform margin (Hunan province, China) from shelf edge collapse products

Abstract

The southeast-facing slope of the Yangtze platform during deposition of the Ediacaran Doushantuo Formation includes several submarine slides and olistostromes of regional extent. These involve shallow-water platform facies, including carbonates, evaporites, and phosphorites. Current-related sedimentary structures and lithofacies allow reconstructing a shelf-marginal, shallow-water, semi-restricted environment (0 to 30 m water depth) near a steep-sided, possibly tectonically defined platform margin inherited from Rodinia breakup.

1. INTRODUCTION

The Ediacaran and Cambrian strata of the Yangtze platform are one of the foremost locations worldwide to study the conditions and setting of the Cambrian bioradiation. A detailed understanding of the temporal sequence and ecologic drivers of this radiation event has been hindered both by a lack of detailed correlation between the numerous important fossil-bearing locations (e.g., Miaohe biota, Hubei Province (Xiao et al., 2002); Weng'an biota, Guizhou Province (Yin et al., 2001; Yin et al., 2004; Chen et al., 2004), Chengjiang biota, Yunnan province (Chen et al., 1991; Chen et al., 1999; Babcock and Zhang, 2001; Babcock et al., 2001; Hou and Bergstrom, 2003; Hou et al., 2004; Shu et al., 2004) and by a poor understanding of the process sedimentology. In the transition zone between the fossiliferous, shallow-water, stratigraphically incomplete carbonate environment and the deep-water, stratigraphically almost continuous but mostly fossil-free siliciclastic environment may lie the potential to reconstruct a detailed stratigraphic account of the tectonic and climatic drivers in the evolution of the Yangtze platform.

The Yangtze platform represents the central part of southeastern China and covers approximately 800,000 km^2. This study focuses on the southern margin of the Yangtze platform in Hunan province where the late Proterozoic slope facies is well exposed, and presents data and interpretations from stratigraphic measured sections.

1.1. Methods

Stratigraphic sections were measured during two field seasons in 2002 and 2003. Approximately 50 representative samples were cut, polished, and commonly scanned in order to highlight sedimentary structures and facilitate facies analysis. Petrographic thin sections aided in the identification of mineralogy, diagenesis, and microfacies analysis. XRD analysis on whole rock samples were used for the determination of sample mineralogy.

1.2. Location and geologic setting

All studied sections are located in Hunan province (Fig. 45), set in the south-facing slope environment of the Yangtze platform during the Ediacaran (Doushantuo Formation) (Fig. 46). Two sections (Wuhe and Xikou) in Guizhou province (see Fig. 53 for location) complete these data.

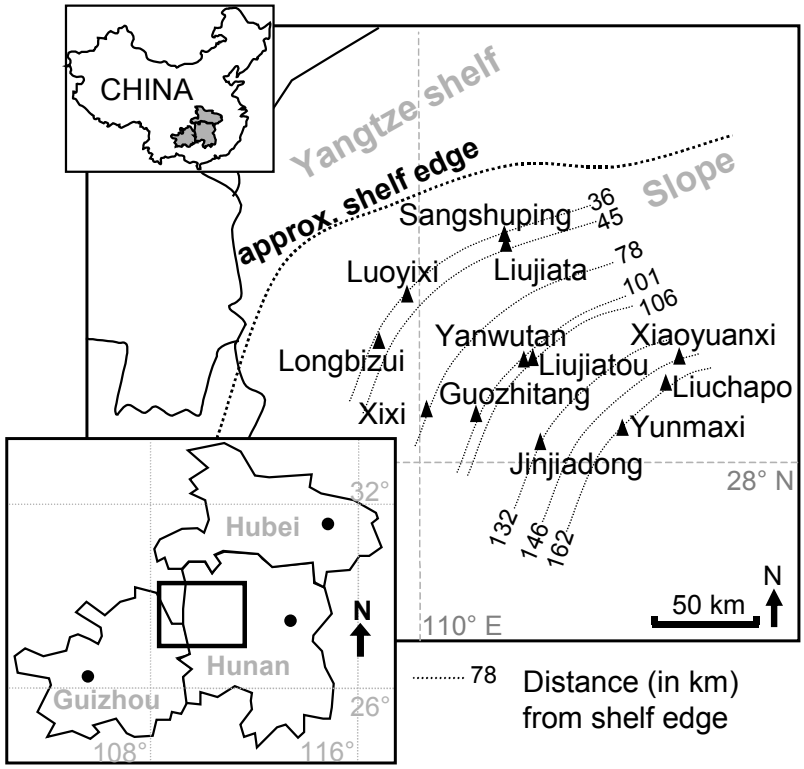

Fig. 45. Geographic and tectonic location of the study area, largely in northern Hunan Province, central China, representing the Ediacaran south-facing slope of the Yangtze craton.

At present, the Yangtze platform is limited to the north by the Qin-Lin fault, extending from Tibet to northern Anhui, and to the southeast by the Cathaysia suture. Its current setting is the result of Yangtze microplate collision with the Cathaysia arc to the SE during the Silurian and with the North China craton to the north during the early Triassic (Kenneth and Cheng, 1999). These collisions deformed the Paleozoic sedimentary cover of the Yangtze platform only moderately. Cretaceous extension created large, fault-bounded basins filled by continental-facies lithologies. Generally, Proterozoic-Paleozoic strata are preserved in a thickness of several kilometres and are moderately and large-scale folded.

The location of the South China craton during the Ediacaran and its place in the Rodinia supercontinent, like that of many other small cratons, is poorly known. Paleomagnetic analysis indicate an equatorial position (Macouin et al., 2004) at 600 Ma. Li et al. (1995) proposed that the South China plate linked Australia with Laurentia from 1 Ga to 700 Ma. Powell and Pisarevsky (2002), in their reconstruction of Gondwana and Laurentia, also join South China with Australia. According to Condie (2003) and Pisarevsky et al. (2003), the Yangtze platform and Cathaysia (southeastern part of present-day China) collided to form the South China craton already during

the Meso- and early Neoproterozoic, before they separated again during Rodinia breakup. Since then, the general tectonic setting was extensional, and the platform evolved as a passive margin since the Ediacaran.

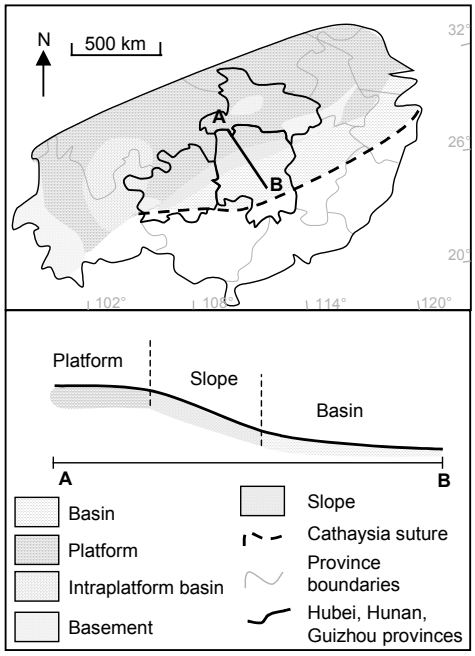

Fig. 46. Paleoenvironmental reconstruction of the southern Yangtze craton during the late Ediacaran (Doushantuo Fm; ~ 635-551 Ma (Condon et al., 2005)) (in part modified after Steiner, 2001).

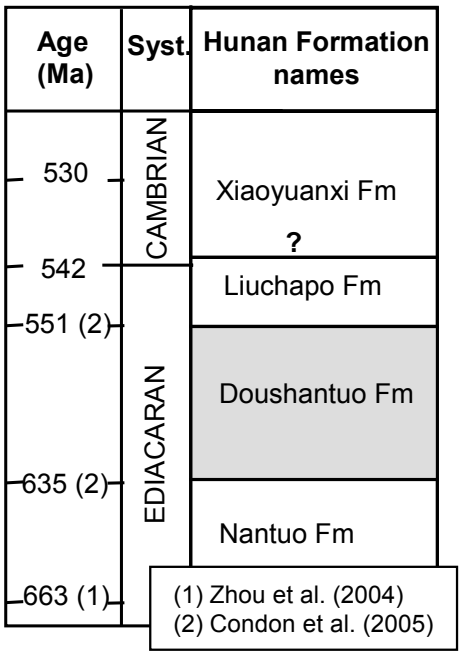

Fig. 47. Schematic stratigraphic column for the Ediacaran and basal Cambrian of south-central China.

1.3. Stratigraphic succession

Formation names change regionally mostly due to lithological and facies changes. Erdtmann and Steiner (2001), Wang and Li (2003), and Zhu et al. (2004) propose a correlation table for the Yangtze platform from the Ediacaran to the Cambrian.

The Ediacaran stratigraphic succession in Hunan province (Fig. 47) begins with the thick diamictites of Nantuo Formation. The glacial character of the Nantuo Formation is locally doubtful (Bahlburg, 2004; Dobrzinski et al., 2004; Eyles and Januszczak, 2004; Dobrzinski and Bahlburg, submitted). Its age is also debated: Evans et al. (2000), Wang and Li (2003), and argue for a Sturtian glaciation (approx. 750 Ma, Frimmel et al., 2002) whereas Jiang et al. (2003c), Chen et al. (2004), and Zhou et al. (2004) propose that Nantuo tillites are time-equivalent to the Marinoan glaciation (approx. 663 Ma, Knoll and Xiao, 1999) The thickness of Nantuo Formation ranges from 0 to more than 2000 m. Its maximum is reported in northern Guangxi province (Wang and Li, 2003). Wang and Li (2003) argue that the Nantuo Formation represents the latest stage of rifting during Rodinia breakup. These partially glaciogenic sediments gathered renewed interest with the “Snowball Earth” theory (Hoffman et al., 1998; Hoffman and Schrag, 2000; Hyde et al. 2000; Runnegar, 2000; Hoffman and Schrag, 2002). A “cap carbonate” of approximately six meters thickness overlies the diamictites and forms the basal unit of the Doushantuo Formation. U-Pb

dating on zircons yields an age of approx. 635,2 +/-0,6 Ma (Condon et al., 2005). These carbonates show unusual sedimentary structures (Sumner, 2002, Nogueira et al., 2003) and a negative $\delta^{13}C$ isotope anomaly (Knoll et al, 1993; Germs, 1995; Corsetti and Hagadorn, 2000), marking a sudden Ediacaran change from icehouse to greenhouse conditions. The Nantuo Formation “tillites” and the Doushantuo Formation “cap carbonate” extend regionally throughout the central and southern Yangtze Platform.

The remaining bulk of the Doushantuo Formation in Hunan province represents a deep-water environment below wave base and is dominated by black, thinly-laminated, more or less silicified suspension-sedimented shales, interbedded with thinly bedded, dark-grey siltstones resulting from turbidity currents, rare, thinly laminated cherts, and with presumably two, regionally traceable phosphorite horizons which are also well developed on the Yangtze platform. Allochthonous shallow-water, dolomitized limestone intervals with current-induced sedimentary structures and gently deformed by soft-sedimentary deformation locally interrupt the autochthonous black shales. They reach up to 60 m in stratigraphic thickness, are oriented nearly conformably with under- and overlying slope facies sediments, and can be correlated through their stratigraphic position, lithology, and facies over large distances (> 50 km). They can therefore be considered as mega-olistoliths or slide sheets. Tuffaceous sediments are common but thin and commonly discontinuous. Most shales contain minor or variable tuffaceous components.

The contact from the Doushantuo Formation to the overlying Liuchapo Formation is drawn at the first occurrence of thick-bedded silicified shales. This contact is commonly erosive. In several sections we examined, it represents the base of a thick allochthonous sequence involving olistostromes and large-scale contorted bedding. The silicified black shales of Liuchapo Formation grade updip into dolomitized limestone of the approximately time-equivalent Dengying Formation, which is widespread in the Yangtze platform-facies of northern Hunan and Hubei Provinces (Fig. 47).

2. DATA

2.1. Sedimentary record of the Doushantuo slope

Slump-folded Doushantuo black shales are interbedded with gently deformed limestones (and phosphorites) above discrete discontinuities and interpreted as olistostromes. The carbon isotopic evolution highlights also the presence of slide sheet in Yanwutan section (Guo et al., in press). Four major slide events are regionally traceable in the slope sections of Hunan province (Vernhet et al., 2004b; Fig. 48). Two-to-30m-thick, these slides mostly involve shallow-water, platform-edge-derived calcareous rocks. Their internal sedimentary sequence is preserved and therefore allows reconstructing the paleoenvironment of the platform edge and its evolution in the time. We focus our study on the largest and thickest of the four mass-flow events, slide No. 3 (Fig. 48) because it occurs in almost all studied sections and shows a broad facies diversity. The facies analysis was supported by approximately 20 hand samples and 30 thin sections. Additional observations on outcrop scale contribute to our conclusions because diagenesis masks a large part of the initial lithology.

2.2. Olistostrome facies description and interpretation

Olistolith lithologies include a variety of dolomite, limestone, marl, chert, and shale. Widespread dolomitization renders the identification of primary lithologies, textures, and structures difficult. The phosphorites do not show any late diagenetic replacement features; however, evaporites are nearly all replaced by calcite or quartz and identifiable as pseudomorphs only.
Lithologies and sedimentary structures can be grouped and assigned to three facies with several subfacies.

2.2.1. Phosphorite / Chert / Evaporite /Dolomite facies association

Facies 1:

Facies 1 is thinly laminated, pink dolomites interbedded with patchy, black, thinly laminated silicified mudstones. Few cm-scale “tepee structures” deform locally the silicified mudstones and are onlapped by cherty beds (Fig. 49A). Internal erosion surfaces are marked by a black laminae (Fig. 49B) or by irregular cherty surfaces. In outcrop, this interval measures 1,50 to two meters thick. The contact with the underlying, deformed, autochthonous black shales is erosive. The contact with overlying, allochthonous, silty, current-related laminated limestones is sharp and parallel. In thin section, the samples show mm-sized radial pseudomorph quartz crystals after gypsum around a nucleus of degraded organic matter. Light beige carbonate or phosphoritic micrite is interbedded with dark bituminous laminations. Patchy apatite cement is rare. This facies is particularly well represented in Luoyixi section (Fig. 49). In Yanwutan section, very fine-grained dolomitized grainstones/packstones are interbedded with silicified evaporitic dolomite/phosphorite.

Early diagenetic silica cementation preserved biolaminations while erosive surfaces indicate periods of emergence. The small-scale onlap indicates that the “tepees” are likely result of early diagenetic sediment dewatering during exposure to atmosphere rather than dewatering during burial. Original organic matter content was apparently high due to microorganisms covering the sediment surface. Hypoxic conditions under the biomats may have allowed the concentration of fluoroapatite and the subsequent precipitation of early-diagenetic patchy phosmicrite. In Yanwutan section, the presence of fine-sand-grained dolomitized grainstones/packstones in the allochthonous block indicates that the original location of the displaced block was subjected to medium-energy currents. In Luoyixi section, the sedimentation style in the allochthonous section is entirely dominated by suspension settling and (bio-) precipitation. Therefore, the slide block of Luoyixi section may have been in a more protected environment than that of Yanwutan, shallow enough to be temporarily emergent and to allow the formation of tepee structures by subaerial dewatering of sediments.

Facies 2:

Facies 2 is characterised by two types of phosmicrite, interbedded with evaporitic dolomicrite (Fig. 50A, 50B, 50C) and subjected to reworking resulting in phosintraclasts, dolomicrite-matrix-supported microbreccia (Fig. 50F), cm-sized phosclasts, and highly deformed dolomicrite-supported breccia (Fig. 50G). In outcrop scale, this phosphoritic interval is approximately 1,5 to

two-m-thick and shows interbedded thin-bedded phosmicrites, microbreccias, breccias, and evaporitic dolomite. This facies is represented in Xixi section.

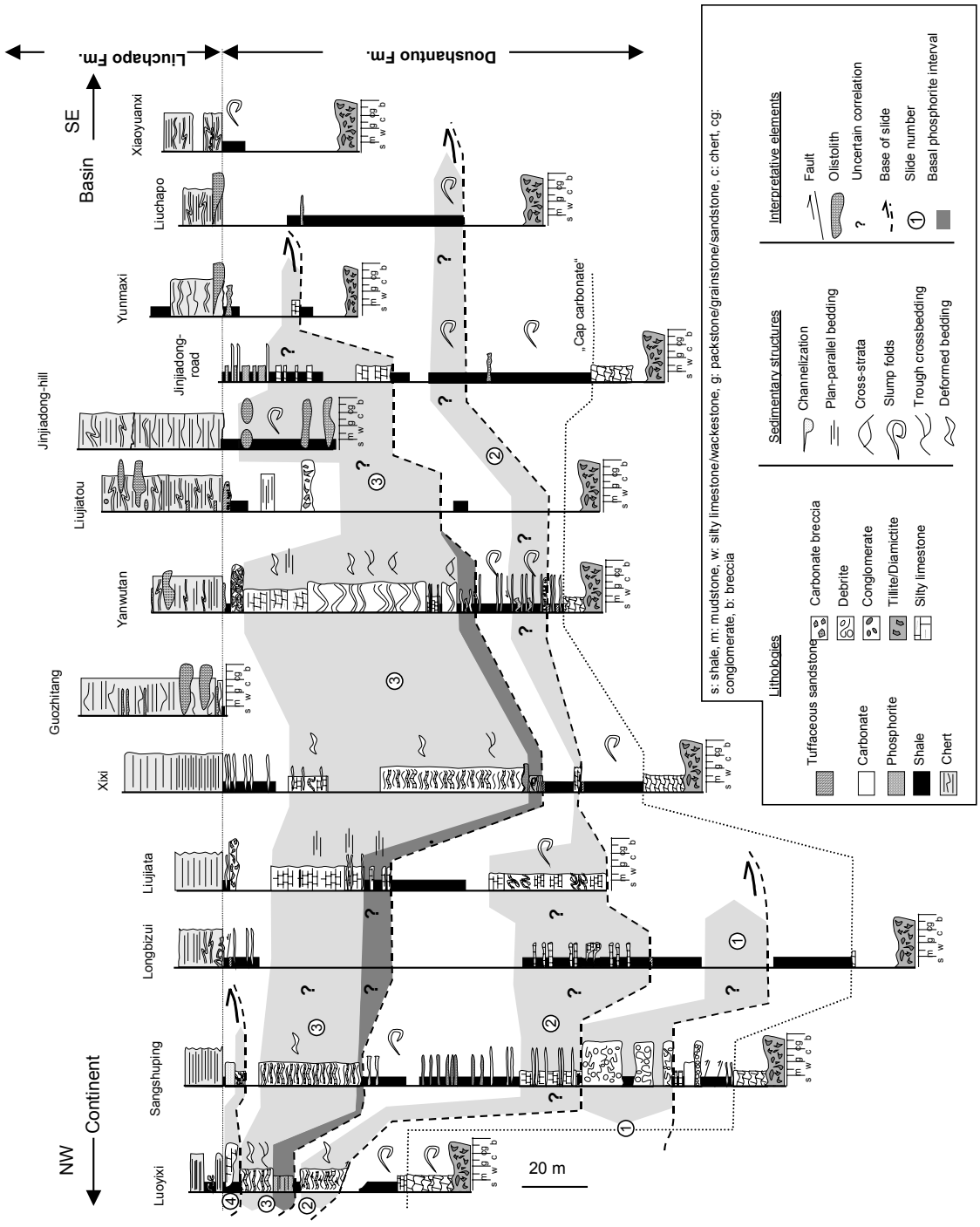

Fig. 48. Stratigraphic correlation diagram between key sections in Hunan province showing SE-ward progradation of discrete mass transport events (slides 1 through 4) on the south-facing slope of the Yangtze platform. See Fig. 45 for location.

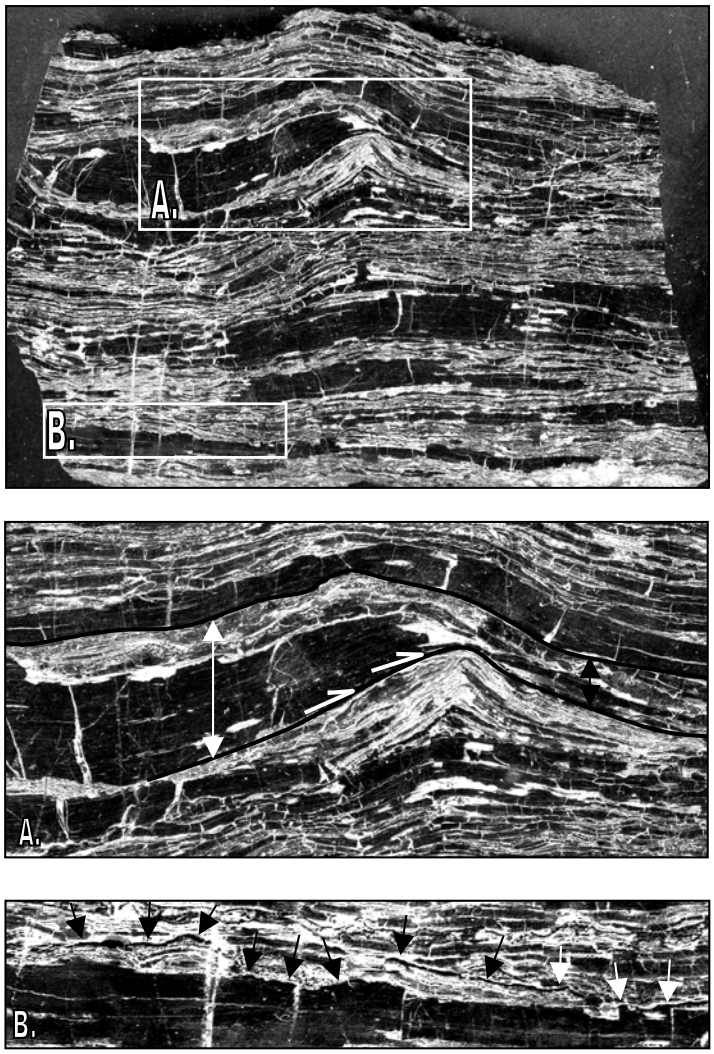

Fig. 49. Facies 1 showing evidence for occasional emergence in Luoyixi section (Hunan province). A. Small-scale thickness variations marking sediment onlap on “tepee structure”. B. Small-scale internal erosion surface marked by possible biomats. Dimensions of the hand sample are 8 cm*12 cm.

The phosmicrites can be grouped as either “soft-phosmicrite” or “hard-phosmicrite”, depending on their response to applied stress. Soft phosphorites show one-to-five-cm-thick beds of reddish-brown, thinly laminated phosmicrite (Fig. 50B, 50C). These show evidence of soft-sediment behaviour, which allowed their mixing with plastically deforming dolomite during brecciation. Thin section examination demonstrates that laminations consist of approx. 200µm-thick couplets of basal organic matter-rich, black biomats overlain by thin phosmicrite. Apatite and calcite-filled spheres, possibly microfossil remnants, interrupt the laminations (Fig. 50D, 50E). The “hard phosmicrites” consist of cm-thick, dark brown to black phosmicrite beds (Fig. 50A, 50B, 50C) including mm-sized, calcite-filled, round, unidentified fossils. Small pyrite crystals are common. These phosmicrites show a brittle behaviour and are the main source of clasts during reworking. In thin section, structureless opaque-brownish micrite is interbedded with thin organic-matter-rich, opaque laminations. The base of beds has a sharp, regular conformable contact with underlying

dolomite or phosphorite. In contrast, their top may be erosional, highlighted by eroded spherical fossils. Biomats cover this surface.

Phosmicrite precipitation requires a low-energy environment with low sedimentation rates and semi-anoxic conditions (Liang and Chang, 1984; Yiqing, 1984; Föllmi, et al. 1991; Trappe, 1998; Trappe, 2001). The interbedding of biomats with phosmicrite is the result of rhythmic sedimentation. Periods of relatively high sediment supply mixed clays with the phosmicrites; biomats covered these beds during period of low sediment supply. The high number of laminations and low bed thicknesses indicates a high-frequency process. The high concentration of fine-grained siliciclastic grains may be due to seasonal precipitation. Alternatively, the variable and rhythmic growth of biomats may also be due to seasonal changes in water temperature, light, and/or chemical conditions. Similar to varves observed in modern lakes, the rhythmic thin beds could be attributed to seasonal rainy/drought periods.
The “hard” phosphomicrites correspond to periods of significant phosphogenesis and organic matter production. Both processes require low sediment supply. Thus, erosion surfaces on the top of the “hard” phosphorite beds argue for a relatively long period of sediment starvation allowing, in a first step, formation of bacterial films on the surface of sediments, which assure semi-anoxic conditions necessary for subsequent phosphogenesis, and, in a second step, erosion of biomats and of a part of the consolidated underlying phosmicrite. Therefore, hard phosphorite beds appear to be small-scale hardgrounds. At hand-sample scale, the internal geometry of the phosmicrites appears to alternate between times of elevated periods of sediment supply (which may have induced the formation of “soft phosphorite” beds) and periods of sediment “starvation” (which allow reworking and eroding the “hard phosphorite”).

“Hard” and “soft” phosmicrites are reworked to micro-breccias and breccias. Micro-breccias (Fig. 50F) show two-to-five-cm-thick beds with approximately half-cm-sized phosintraclasts in a dolomite matrix. The dolomite matrix shows an irregular, complex network of curved, calcite-filled fractures. Contacts between the microbreccia and underlying phosmicrite are erosive. In thin section, fractures in the dolomicrite matrix appear to be part of mm-sized collapse breccias and small-scale enterotrophic structures by coalescence of small-scale evaporite nodules. Structureless fine-grained phosmicrites constitute the intraclasts.
Microbreccias represent short-distance transport of phosmicrite hardground chips, eroded by currents. They may record occasional storms in a dominantly low-energy environment. Dolomicrite-mud-matrix-supported breccias (Fig. 50G) include cm-sized phosmicrite hardground intraclasts which may be aligned and define decimetre-sized tight folds. The matrix is veined by an irregular, complex network of small-scale (mm-sized), curved fractures filled by calcite, which gives the lithology a highly deformed appearance.

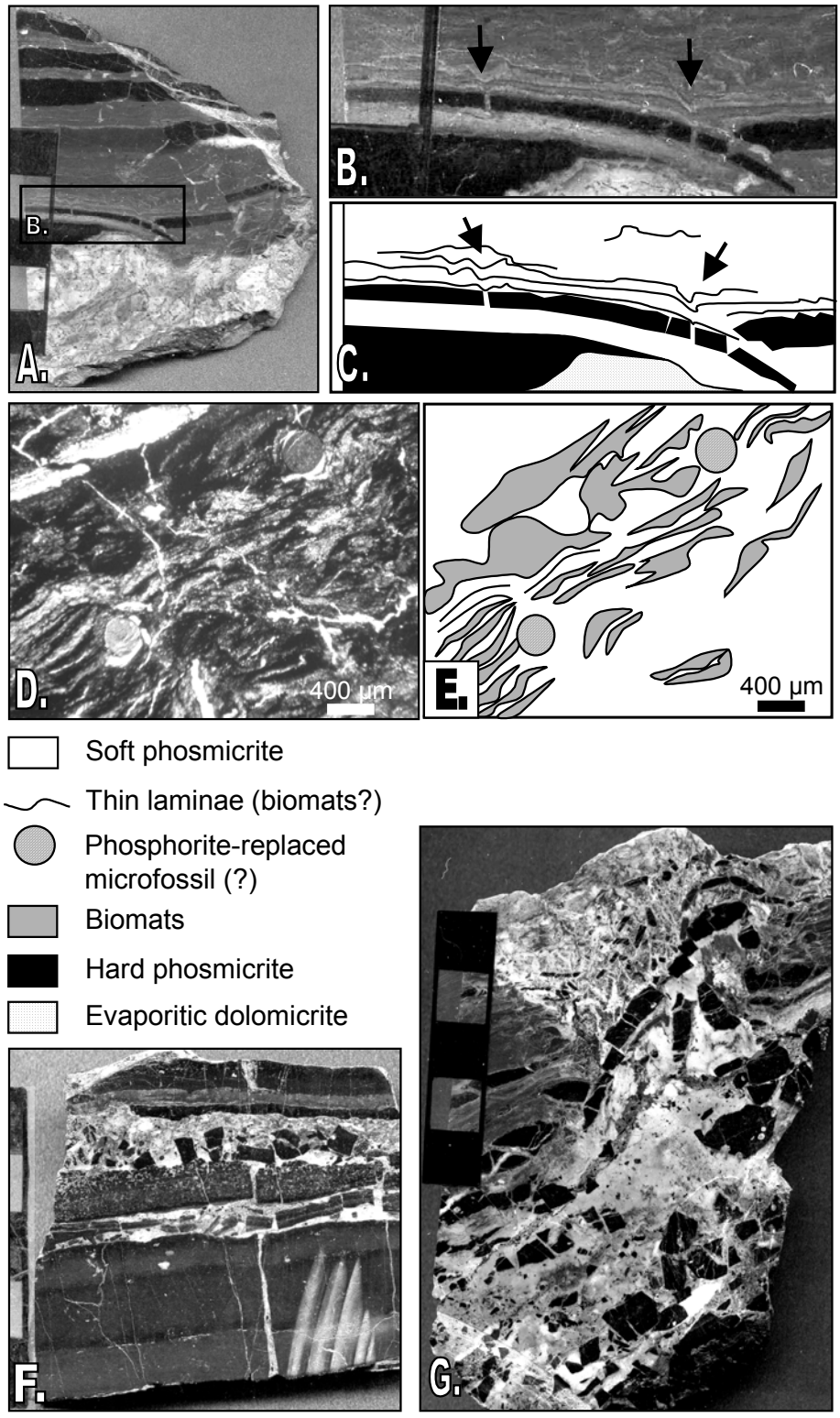

Fig. 50. Facies 2; samples from Xixi section, Hunan Province. A, B, and C: Hand samples and interpreted line drawings showing internal structures of soft phosmicrites. Biolaminations deform plastically (black arrows) while black, hard phosmicrites deform brittily. D and E: Thin section photomicrograph (D) and line drawing of "soft phosmicrite". Spherical microfossils (?) interrupt biolaminations. F: Microbreccia with half-cm-sized clasts of phosphorite hardground ("hard phosmicrite"). Scale bar is 5 cm long. G: Tight fold defined by cm-sized phosphorite-clast breccia hardground ("hard phosmicrite") due to precipitation and dissolution of evaporites in a dolomicrite matrix. Scale bar is 5 cm long.

In the 15 samples examined, the phosphorite hardground represents variable degrees of deformation, ranging from thin fractures to complete disorganization of the bed. In thin section, palisade calcite (possibly replaced palisade gypsum) commonly surrounds phosphorite clasts. Acicular and lozenge-shaped pseudomorph calcite after gypsum and anhydrite crystals are common. 0,5-to-one-cm-thick, “contoured” calcite veins without preferential orientation, and cm-thick collapse breccias are abundant (Fig. 51).

The presence of pseudomorph evaporitic crystals suggests that brecciation may be related to primary or early diagenetic evaporite crystal growth and dissolution (Fig. 56). As a result, the competent phosmicrite beds fractured to accommodate the deformation. Semi-consolidated dolomicrite mud flowed into these fractures and facilitated subsequent deformation.

2.2.2. “Silty dolomitized limestones and grainstones/packstones with current-related sedimentary structures” facies association

Facies 3: Facies 3 usually overlies Facies 1 and 2 of the phosphorite / evaporite / dolomite / “chert” association. At outcrop scale, this interval ranges from approx. five-to-30m-thick and consists of silty dolomitized limestones, grainstones, or packstones with current-related crossbedding and various types of laminations. The strata are gently deformed by secondary deformation, possibly due to soft-sedimentary slumping. This facies can be subdivided in subfacies according to their depositional conditions, determined from preserved sedimentary structures at outcrop scale.

Sub-facies 3A: This facies shows three to ten cm-thick, normally graded packstones organized in plan-parallel, cm-thick units (e.g. Xixi section) or silty dolomitized limestones with trough crossbedding (e.g. Luoyixi section) (Fig. 52A).

Sub-facies 3B: This facies includes 0,5m-to-one-m thick, thick-bedded cross-stratified dolomite grainstones/packstones (e.g., Yanwutan section). In thin section, this facies shows secondary euhedral dolomite rhombs with some pyrite crystals, rendering the identification of the primary microfabric impossible (Fig. 52B).

Sub-facies 3C: This facies consists of medium-sand-grained dolomite with trough, medium-scale cross-strata. In thin section, euhedral, well-developed crystals of secondary dolomite mask the primary lithology of this interval; however, the sedimentary structures argue for a grainstones facies (e.g. Yanwutan section) (Fig. 52C).

Facies 3 shows characteristic facies associations of a wave- and storm-dominated platform. The association of facies developing shallow-water, plan-parallel sedimentary structures implicates that sub-facies 3A is due to sediment winnowing. Wave-related currents formed sand waves, which are expressed as trough crossbedding in vertical profile. These sediments were deposited in an almost permanently wave-agitated environment. Facies 3B records medium-energy, permanent currents, which move sand-sized particles as bedload and accumulate them in sand shoals. Tidal or coastal currents may have formed these shoals. These banks show mobility and a low lateral continuity, which makes their correlation between outcrop sections difficult. Recent examples in

the Atlantic Ocean, Celtic Sea and North Sea (Reynaud et al., 1999; Trentesaux et al., 1999; Oertel and Overman, 2004) form at maximum 60 m water depth but can occasionally become partially emergent.

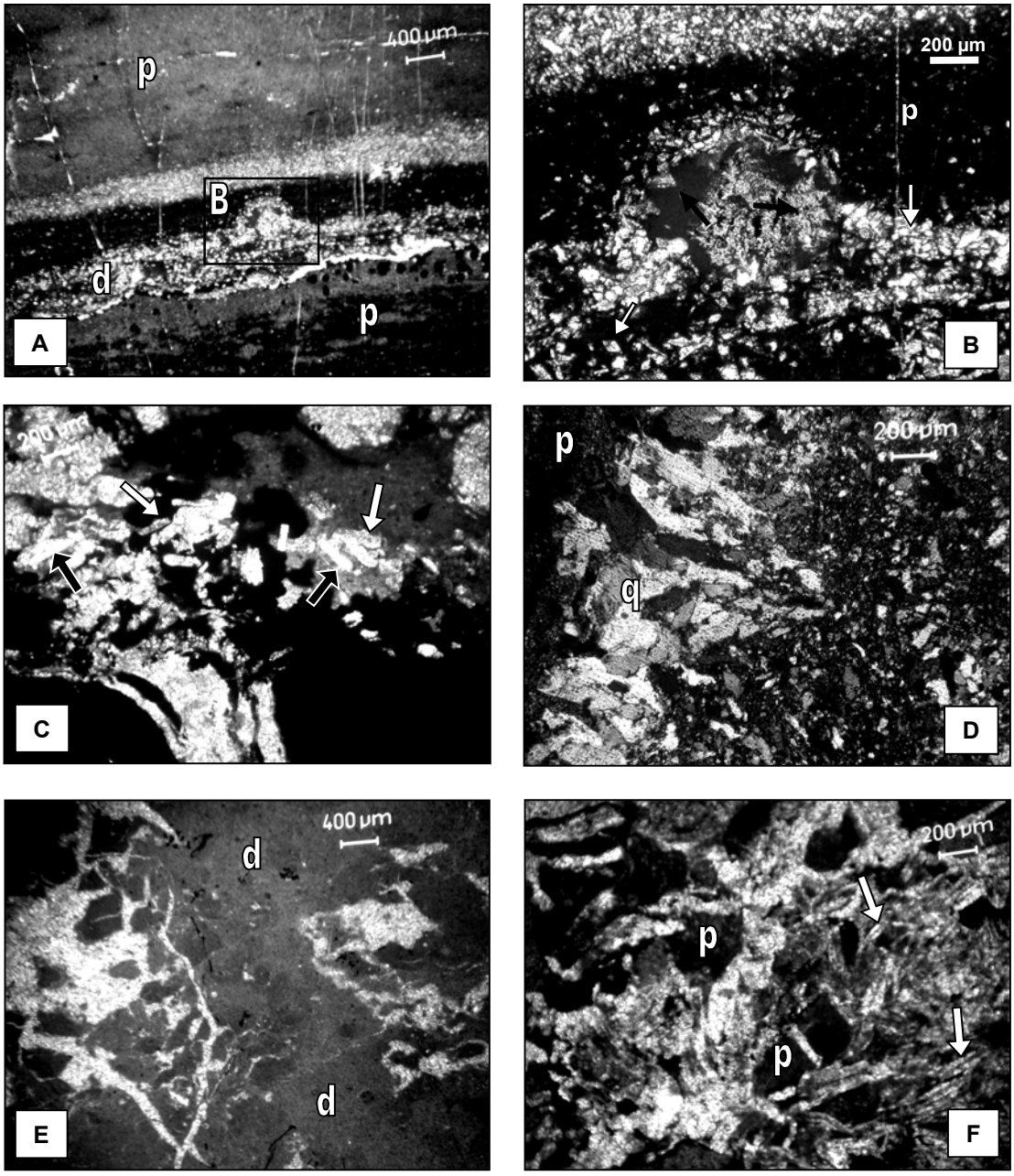

Fig. 51. Evaporites of facies 1 and 2 and their pseudomorphs in thin section from olistoliths in Xixi section (except D: Luoyixi section). A. Microdome of fan-shaped gypsum pseudomorphs (Facies 2). B. Detail of A. Note radial growth of calcite replacing gypsum (black arrows) and the well developed, euhedral dolomite crystals (white arrows; Facies 2). C. Anhydrite pseudomorphs after gypsum (white arrows) and calcite pseudomorphs after gypsum (black arrows) in evaporitic dolomicrite-supported breccia (Facies 2B). D. Large quartz crystals replacing gypsum (Facies 1). E. Evaporitic dolomicrite matrix with (to the right) small-scale, calcite-filled fractures organized in enterotrophic (coalescent small-scale nodules) structures and small-scale collapse breccia (left) due to local dissolution of evaporites (Facies 2B). F. Calcite cement replacing anhydrite. Note the acicular crystals between phosphorite intraclasts (Facies 2B). p : Phosphorite, d : evaporite-bearing dolomite.

Facies 3C resulted from high-energy currents induced by storm events, which form small-scale dunes on the sea floor recorded in the sediments by medium-scale through crossbedding. All three subfacies represent shallow-water environments between five and 60 m water depth.

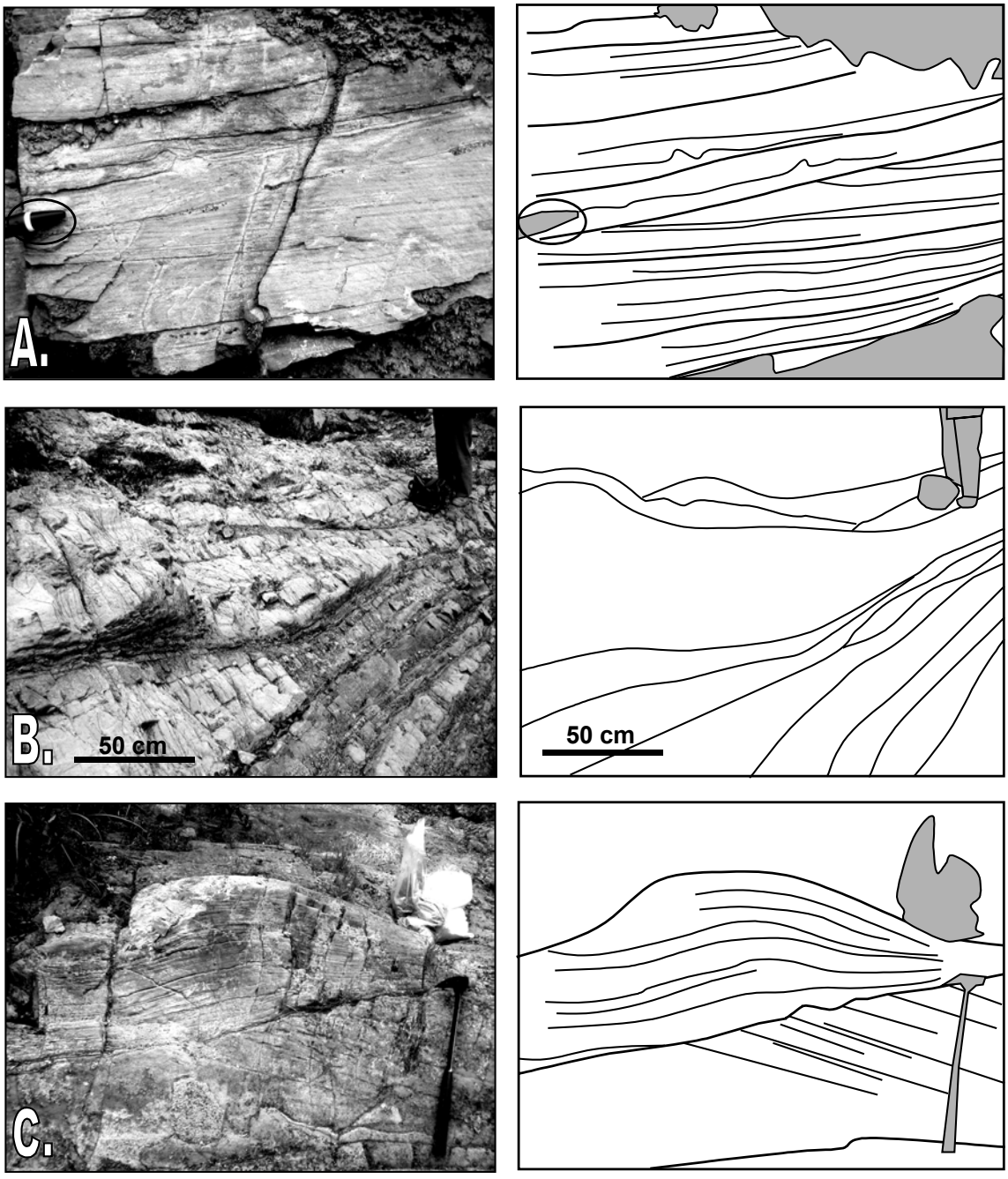

Fig. 52. Outcrop view of Facies 3. A. Silty dolomitized limestones with trough cross-laminations deposited above the fair-weather wave base. Pen tip ~ 2 cm long; Luoyixi section. B. Large-scale cross-strata with internal crossbedding representing sand shoals. Scale is 50 cm long; Yanwutan section. C. Crossbedding formed by mega-ripples. Hammer for scale is 40 cm long; Yanwutan section.

2.3. Depositional environments

2.3.1. Phosphogenesis in shallow-water, restricted basins

Phosphogenesis generally requires semi-anoxic environments. These allow, on one hand, the accumulation and preservation of organic matter (Baturin, 1982) and, on other hand, its partial degradation, allowing phosphate to saturate the pore water (Trappe, 1998; Schwennicke et al., 2000). Therefore, sedimentation of phosmicrites requires a low-energy environment in which the water column remains stratified, causing precipitation of apatite in the uppermost ten cm of the sediment (Föllmi et al., 1991). In addition, phosphorites in this study are associated with biomats and mudstones, which may have acted as impermeable barriers and prevented fluid exchange with oxygenated water (Schwennicke et al., 2000). Moreover, microbial activity favours phosphogenesis by degradation of organic matter (Föllmi et al., 1991; Trappe, 1998), thereby providing a proximal source of Phosphorus. The phosmicrites in the study area were therefore likely deposited in a restricted basin with high organic matter content and semi-anoxic conditions. Laminations in the phosmicrite suggest the presence of bacterial and algal mats. The episodic deposition of thin evaporitic dolomicrite indicates temporary evaporative conditions and records rhythmic variations of the sedimentation rate in the succession of phoscrete hardgrounds, evaporitic dolomitized limestones, and clay-rich phosmicrites colonized by biomats.

2.3.2. Shallow-water, wave-dominated platform

High-energy, open-marine, crossbedded sand shoal deposits overlie the phosphoritic facies and indicate that a “barrier”, protecting a restricted low-energy intra-shelf basin, was removed, allowing coastal and/or tidal currents to act on the platform, to remove the sediments, and to allow sand sedimentation. The associated sedimentary structures indicate a water depth range from five to 60 m. The predominance of winnowed and trough crossbedding suggests a shelf water depth near the fair-weather wave base (30 m). Thus, the edge margin of the southern part of the Yangtze platform may have been wave-dominated during the middle part of Doushantuo Formation.

The Yangtze platform shelf edge shows shallow-water environments facing the shelf and deep-water environments facing the slope. This transition seems sharp and abrupt, and no transitional facies have been reported in the literature.

2.4. Platform-margin collapse structures in Guizhou province

Numerous allochthonous slide blocks are readily recognizable in the shale-dominated sedimentary record of the Doushantuo Formation slope sections because the blocks involve shallow-water carbonate facies. Other olistromal deposits appear to occur for several 100 km westward into Guizhou Province (Fig. 53).

An approximately ten-m-thick olistolith in Wuhe section, Guizhou Province, is located near the top of the Doushantuo Formation. The block consists of brown-beige, cm-thick, interbedded dolomitized mudstones/wackestones /packstones, with desiccation cracks structures forming polygons on bedding surfaces. A three-cm-thick bentonite overlies the carbonate blocks and separates it from autochthonous cherts and silicified shales of the overlying Liuchapo Formation.

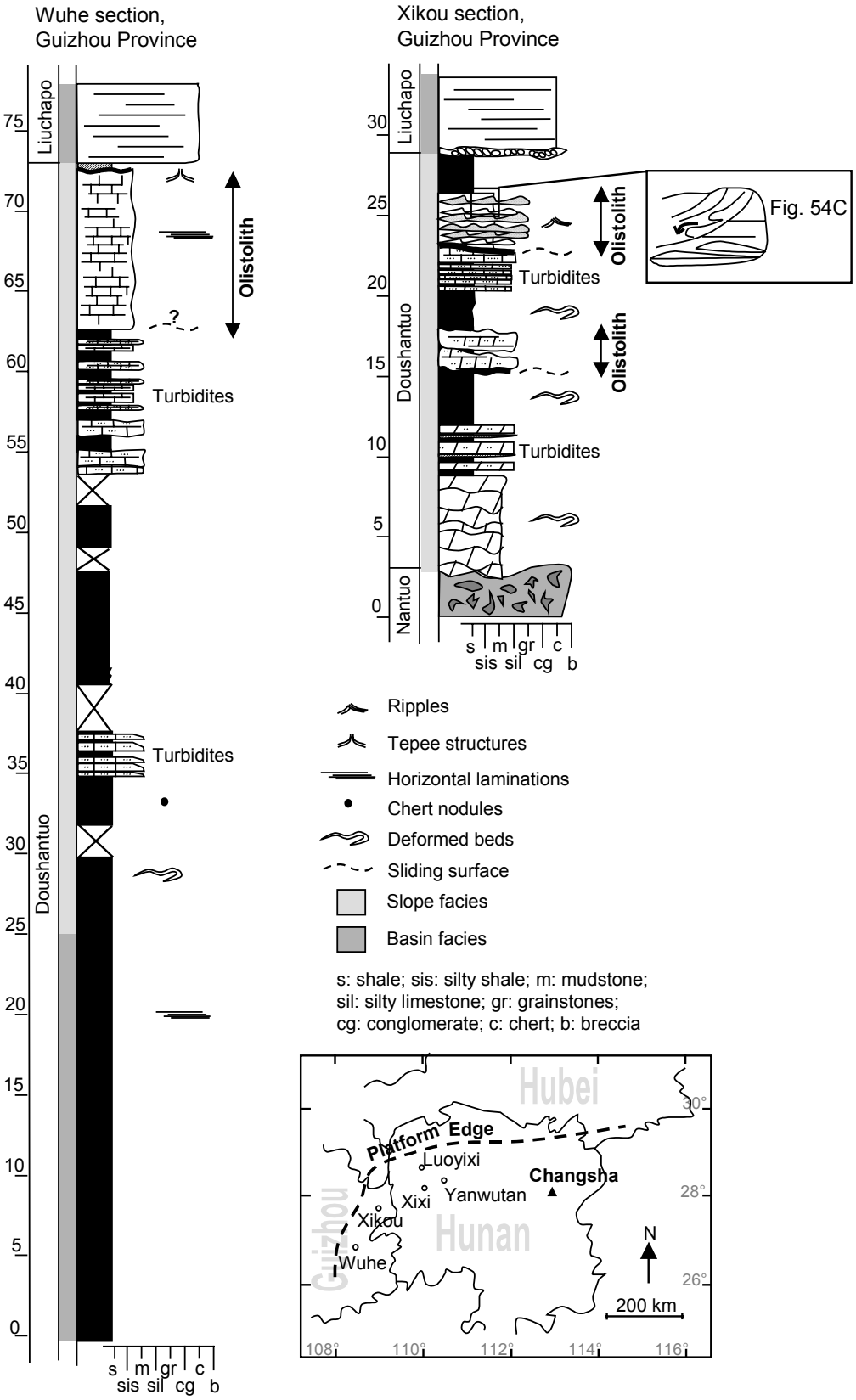

Fig. 53. Stratigraphic columns of Wuhe and Xikou sections, Guizhou province, documenting the presence of olistoliths with shallow-water platform facies in the slope facies.

The approximately 60-m-thick underlying autochthonous section consists dominantly of shales. Its depositional environment is difficult to determine due to the absence of identifiable sedimentary structures. However, deformed beds approximately 30 m above section base and the presence of an olistolith argue for a slope environment, possibly underlain by basin facies. The base of the section is poorly exposed (Fig. 53). The base of Xikou section, Guizhou Province, exposes Nantuo Formation diamictites and a five-m-thick “cap dolomite” with slump structures, overlain by 20-m-thick shales and turbidites. Two olistoliths interrupt the suspension- and turbiditic sedimentation. The lower block, approx. 15m from the base of the section, involves silty limestones (Fig. 54A). Its shallow-water character is not evident. The second olistolith, above an erosive contact with the underlying turbidite deposits (Fig. 54B), occurs ten meters higher and shows sigmoidal climbing ripples, involving fine-grained grainstones to packstones and wackstones with common sedimentary structures that most closely resemble structures formed in tidally-influenced environments and draped by mudstones, thinly laminated by biomats (Fig. 54C). Intraformational channels cut and erode the set of climbing ripples. Purple shales with microbial structures, followed by Liuchapo Formation chert overlie the slide block. We interpret the entire section of the Doushantuo Formation in Xikou section as a submarine slope, affected by mass wasting.

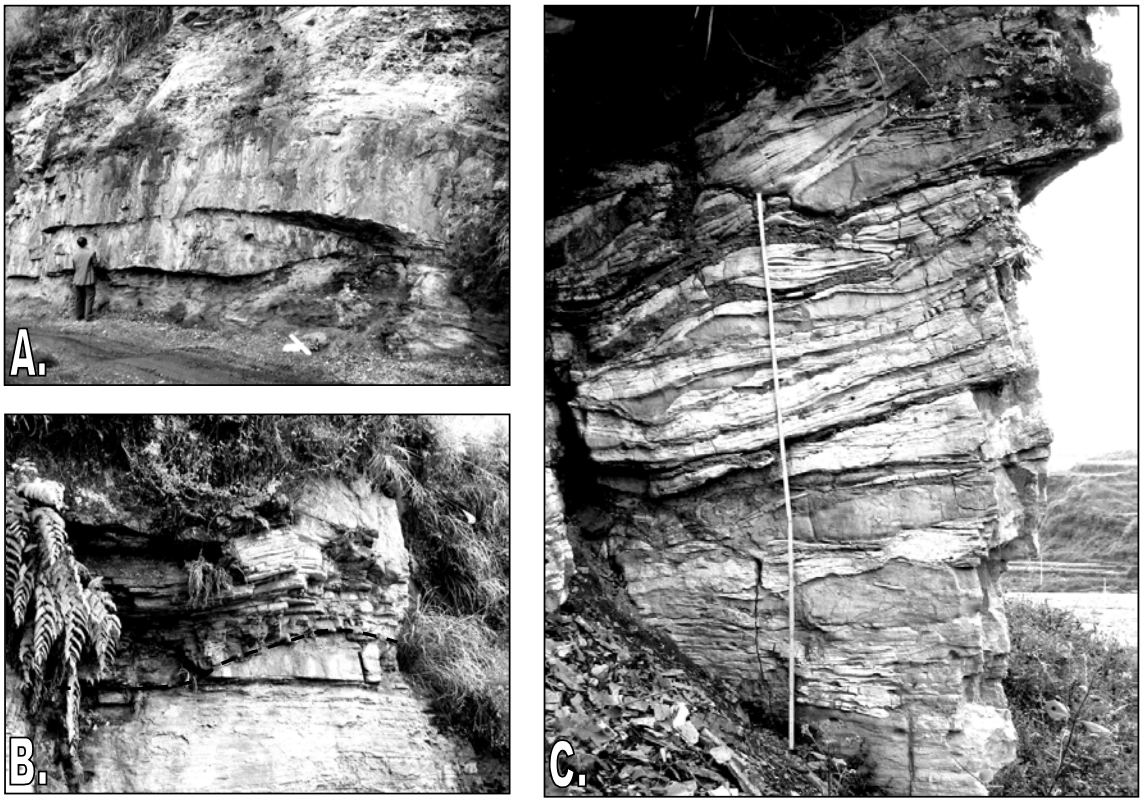

Fig. 54. Outcrop photographs of olistoliths at Xikou section, Guizhou province. A. Lower olistolith involving silty limestones. Note the lenticular shape and the highly deformed surrounding black shales. B. Erosive base of the upper olistolith. The shelf-edge-derived block is in erosional contact with autochthonous slope sediments. C. Complex climbing-ripple crossbedding in the upper olistoliths, attributed to intertidal environment.

3. DISCUSSION

3.1. Relative dating of slides

The slope sedimentation process by displacement of large slide sheets limited their internal deformation and largely conserved the original stratigraphy of these platform edge deposits (Vernhet et al., 2004b) (Chapter 4). Therefore, a correlation of allochthonous olistostrome-internal stratigraphy with the autochthonous platform stratigraphy may identify that stratigraphic interval of the Doushantuo Formation represented by olistoliths. This would therefore establish a maximum age of mass wasting. The best exposed and almost continuous shelf stratigraphic section for such a comparison is Zhancumping section in Hubei province, located on the south-central Yangtze platform approx. 150 km north of the reconstructed shelf edge (Fig. 55).

Lithologies and depositional conditions at Zhancumping can possibly be correlated regionally with those in slide sheet No. 3 (Fig. 55). Thickness (several m to tens of m) and systematic variations in interpreted depositional environments in the Doushantuo Formation argue for second-order parasequences, which record relative sea level variations due to major tectonic movements rather than short-term climatic changes. Sedimentary packages are separated by erosive surfaces in Zhancumping section and by major facies shifts in Hunan slope sections, interpreted as sequence boundaries.

Allochthonous slide blocks in Luoyixi, Xixi and Yanwutan sections each show facies shifts between the evaporitic/dolomicrite/phosphorite/chert facies association and overlying silty dolomitized limestones with current-related laminations. This facies change marks the transition from a restricted shallow-water basin to a medium-energy shallow-water shelf. The top of the phosphoritic interval may represent a sequence boundary. The similitude in the sedimentary record of Zhancumping section and and of the slope sections indicates that most olistoliths contain the top of the parasequence I and a major part of parasequence II. Major mass wasting at the shelf edge may have occurred during the regressive period of parasequence II. In contrast to olistoliths of Hunan province, lithostratigraphic correlation in the sections studied in Guizhou province is not possible. The slide blocks there may represent middle or upper Doushantuo Formation shelf-edge facies.

3.2. Implications of evaporites

Primary evaporites may precipitate in shallow-water, enclosed continental lakes under hot climate, in saline ponds on Antarctic ice, in deep-water protected basins, or in coastal sabkhas (Cojan and Renard, 1997). The distinction between primary and secondary evaporites is problematic (Blatt, 1992). In the studied sections within the allochthonous slide blocks, the presence of shallow-water facies (Facies 3) overlying an evaporitic dolomite/phosphorite facies association (Facies 1 and 2) allows the interpretation of deposition in a shallow-water, restricted basin. The lack of preferential crystal orientation argues in favour of the primary character of evaporites (Tabakh et al., 1999), at least in Xixi section. The irregular biomat surfaces may have supported the nucleation of evaporite crystals (Kendall, 1992). Apparently, shallow-water, enclosed basins evolved under a semi-arid climate with episodic evaporation, allowing water to become oversaturated with respect to sulfates. Hand-sample inspection suggests four steps in the formation of the phosphorite breccias

in Xixi section. We interprete the brecciation to be due to the ductile flow of plastic evaporitic dolomite under low stresses, deforming overlying sediments (Fig. 56) during precipitation or dissolution of evaporites.

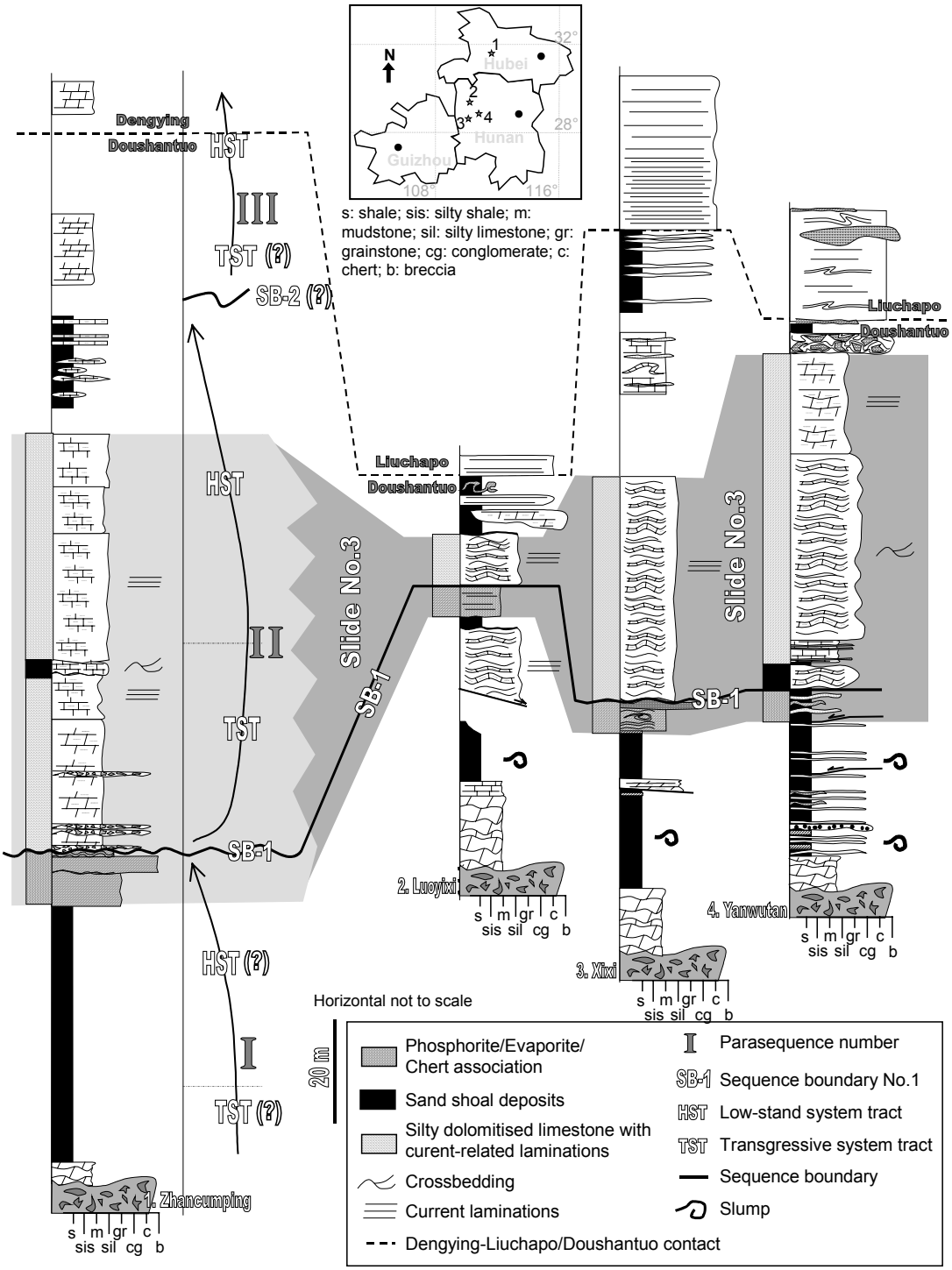

Fig. 55. Comparison between Zhancumping section, Hubei province, and the internal stratigraphy of slide sheet No. 3 (compiled from Luoyixi, Xixi and Yanwutan sections, Hunan province). Second-order sequence analysis supports correlation of the partial sedimentary record in the allochthonous sections with the autochthonous record in Zhancumping section. The olistolith section may correspond to the top of parasequence 1 and the nearly all of parasequence 2.

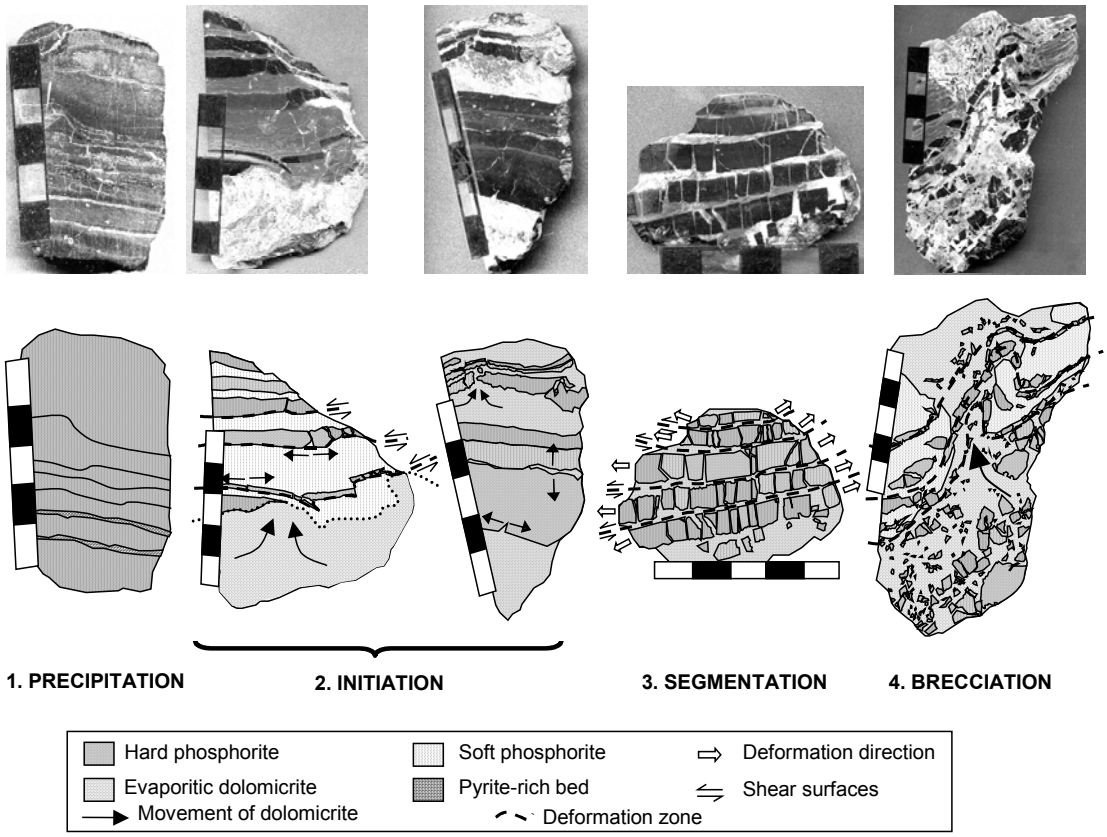

Fig. 56. Stages of evaporite-mediated breccia formation from hand sample (Xixi section, Hunan Province). (1) Initial phosmicrite, formed by concentration of dissolved fluoroapatite in the pore water and precipitation in the uppermost ten cm of unconsolidated sediment under hypoxic conditions due to protective biomats. (2) Ductile deformation. Evaporitic dolomicrite deforms plastically the "soft" phosmicrite. "Hard" phosmicrite hardground, in contrast, accommodates deformation by small fractures perpendicular to bedding. Figures 50 B and C show deformation of (bio?) laminations by brittle segmentation of the black, "hard phosphorite", beds. (3) Brittle segmentation. Evaporitic dolomicrite matrix fills fractures and increases the fragmentation of "hard" phosmicrite, isolating cm-sized clasts. (4) Deformation. Evaporite diagenesis, dewatering, and sediment compaction produce rotated clasts and folds.

3.3. Paleoenvironmental evolution of the platform edge

Fault-controlled blocks inherited from the rifting phase (Wang and Li, 2003) or peritidal sand banks may have contributed to (partially or completely) isolate several shelf-margin mini-basins. In them, evaporites and phosphorites found a variety of depositional environments as a function of water depth, storm activity, seasonal variations in temperature and precipitation, and salinity. With sea level rise, barriers became ineffective. Shelf-edge currents reworked existing sediments and deposited coarse-grained carbonates and local sand banks. Our proposed evolution of the shelf edge (Fig. 57) is consistent with the evolution of more proximal shelf environments in Hubei and northern Hunan provinces (Vernhet and Heubeck, 2004). Several mechanisms such as high pore-water pressure, formation of gas hydrates, sea level fall, and injection of volcanic gases may have caused the initiation of olistostromes and slide sheets. Sliding may have been facilitating by the well-stratified sediments resulting from the absence of bioturbation (Vernhet et al., 2004; Heubeck et al., 2004).

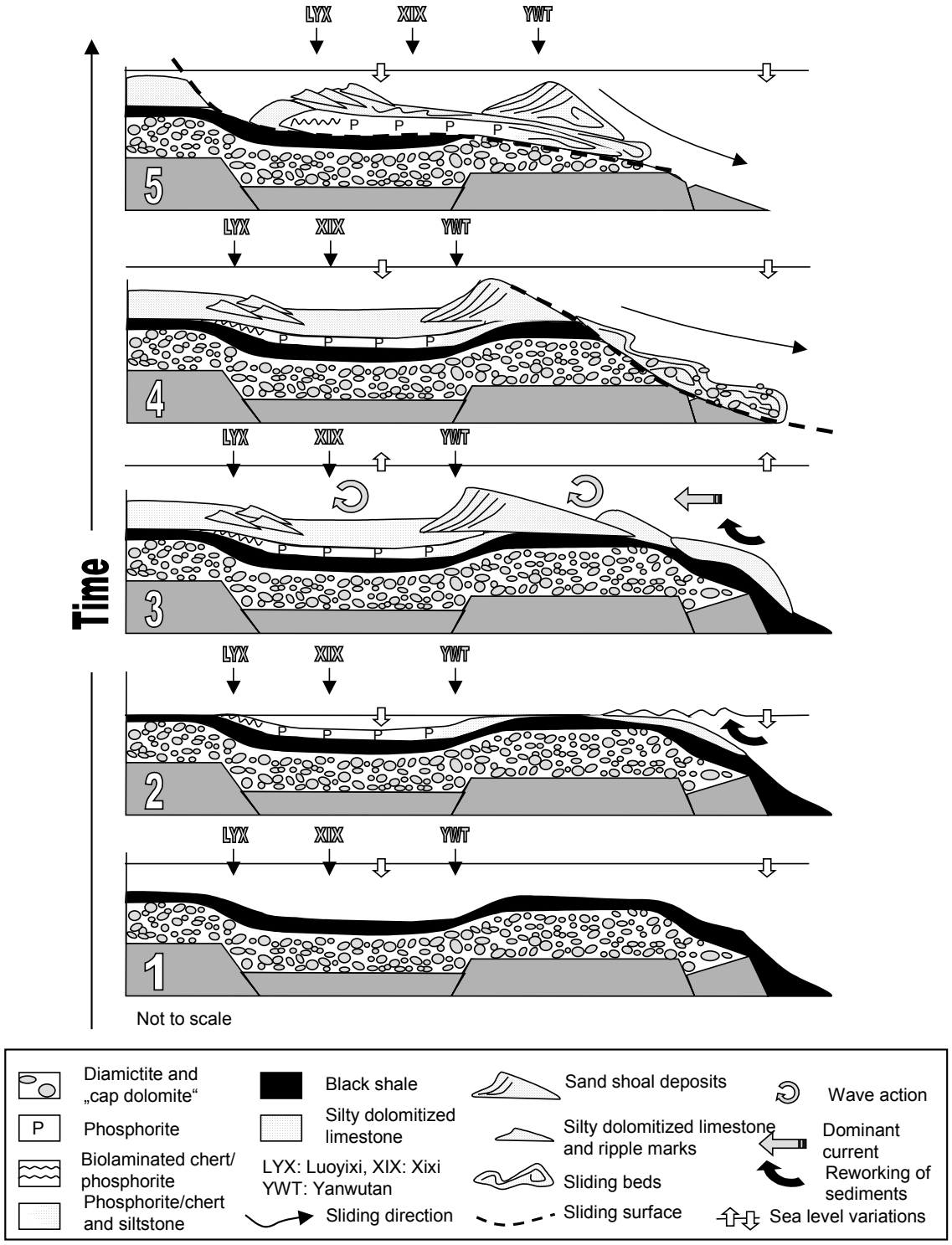

Fig. 57. Possible mechanism and sequence of slide initiation at the south-facing platform shelf edge in Hunan and eastern Guizhou province. (1) Latest rift stage and beginning of thermal subsidence. Marinoan diamictites, “cap dolomite” and Doushantuo black shales fill a tectonically controlled bathymetry. (2) Phosmicrites are deposited during sea-level low-stand in (a) shallow-water, enclosed intra-shelf basin(s) subjected to occasional storms. (3) Barriers become ineffective with sea level rise, and shelf-edge currents rework sediments and deposit coarse-grained carbonates. (4) Sliding of slide sheet No. 2. (5) Sliding of slide sheet No. 3.

4. CONCLUSIONS

Depositional environments along the southern shelf edge of the Yangtze platform, reconstructed in part from large slide blocks on the south-facing submarine slope, show the following features:

1. The platform edge in Hunan and eastern Guizhou provinces, represented in part by allochthonous slide sheets and olistostromes, shows unusual facies, ranging from shallow-water, restricted basin with episodic evaporitic conditions to medium-energy, wave-dominated, shallow-water carbonate platform.
2. The internal stratigraphy of the allochthonous slide sheets may be correlatable with the autochthonous platform stratigraphy and pinpoint the timing of major mass wasting during a regressive period.
3. The parasequences recorded in a shelf stratigraphic column (Zhancumping section, Hubei province) may be correlatable at basin scale and may represent second-order variation of eustacy due to major tectonic events.